SEASONAL CHANGE OF WEPP ERODIBILITY PARAMETERS FOR TWO FALLOW PLOTS ON A PALOUSE SILT LOAM

D. K. McCool, S. Dun, J. Q. Wu, W. J. Elliot, E. S. Brooks

ABSTRACT. *In cold regions, frozen soil has a significant influence on runoff and water erosion. In the U.S. Inland Pacific Northwest, major erosion events typically occur during winter as frozen soil thaws and exhibits low cohesion. Previous applications of the WEPP (Water Erosion Prediction Project) model to a continuous bare tilled fallow (CBF) runoff plot at the Palouse Conservation Field Station (PCFS) in southeastern Washington State showed that WEPP reproduced the occurrence of the large erosion events, but the amount of sediment yield was either under- or overestimated. The inability of WEPP to reproduce the magnitude of field-observed erosion events at the PCFS suggests the need for an examination of the dynamic changes in soil erosion properties and for improving the representation of such dynamics. The objective of this study was to evaluate the seasonal changes of rill erosion parameters for two CBF runoff plots at the PCFS. Field-observed runoff and erosion events during 1984-1990 were used to estimate WEPP hydraulic and erosion parameters, including soil effective hydraulic conductivity, critical shear stress (τ_c), and rill erodibility (K_r). The parameters for each event were best-fitted using WEPP single-event simulations to reproduce the observed runoff and sediment yield on both plots. The results suggest that the adjustment factors for τ_c and K_r of frozen and thawing soils in the WEPP model could be modified to better describe the changes of these parameters in winter.*

Keywords. *Critical shear, Frozen soil, Rill erodibility, Soil erosion, Thawing soil, WEPP.*

Soil freeze and thaw has a significant influence on runoff and water erosion in cold regions (Zuzel et al., 1982; Seyfried and Flerchinger, 1994; McCool et al., 2006). Frozen soil can reduce infiltration capacity (McCauley et al., 2002), and the freeze-thaw processes degrade soil cohesive strength (Kok and McCool, 1990) and increase soil erodibility (Van Klaveren and McCool, 2010). In the Inland Pacific Northwest of the U.S., major erosion events typically occur over large areas during winter from long-duration, low-intensity rain, snowmelt, or both as frozen soil thaws and exhibits low cohesion, and in the summer over small areas from infrequent but intense rainstorms (Horner et al., 1944; McCool et al., 2006).

The Water Erosion Prediction Project (WEPP) model is a physically based simulation tool for water erosion and has been widely used for conservation planning on agricultural, range, and forest lands (Flanagan et al., 2007). WEPP estimates runoff and sediment yield by simulating major hydrological processes, including infiltration, ET, surface runoff, and subsurface flow, and major erosion processes, such as interrill erosion, rill erosion, and sediment deposition (Flanagan and Livingston, 1995). The model also includes a winter hydrology component to simulate snow accumulation and snowmelt, as well as soil freeze and thaw for winter runoff and erosion simulation (Flanagan and Nearing, 1995; Dun et al., 2010).

Previous application of WEPP to a continuous bare tilled fallow (CBF) runoff plot at the Palouse Conservation Field Station (PCFS) in southeastern Washington (Dun et al., 2010) showed that the WEPP model reasonably reproduced the observed snow accumulation and snowmelt, soil freeze and thaw, runoff, and the occurrence of the major observed erosion events, but the sediment yield was either under- or over-predicted. The inability of WEPP to reproduce the magnitude of field-observed erosion events at the PCFS suggests the need for an examination of the dynamic changes in soil erosion properties and for improving the representation of such dynamics.

Elliot et al. (1989) summarized a rainfall simulation study intended to estimate soil erodibility for the WEPP model on 33 soils throughout the U.S. One of the rainfall

Submitted for review in June 2012 as manuscript number SW 9806; approved for publication by the Soil & Water Division of ASABE in February 2013. Presented at the 2011 Symposium on Erosion and Landscape Evolution (ISELE) as Paper No. 11066.

Mention of company or trade names is for description only and does not imply endorsement by the USDA. The USDA is an equal opportunity provider and employer.

The authors are **Donald K. McCool, ASABE Fellow**, Research Agricultural Engineer (Retired), USDA-ARS Land Management and Water Conservation Research Unit, Pullman, Washington; **Shuhui Dun, ASABE Member**, Postdoctoral Research Associate, and **Joan Q. Wu, ASABE Member**, Professor, Department of Biological Systems Engineering, Puyallup Research and Extension Center, Washington State University, Puyallup, Washington; **William J. Elliot, ASABE Member**, Research Civil Engineer, USDA Forest Service, Rocky Mountain Research Station, Moscow, Idaho; **Erin S. Brooks**, **ASABE Member**, Research Assistant Professor, Department of Biological and Agricultural Engineering, University of Idaho, Moscow, Idaho. **Corresponding author**: Donald K. McCool, USDA-ARS Land Management and Water Conservation Research Unit, Department of Biological Systems Engineering, Washington State University, Pullman, WA 99164-6120; phone: 509-335-1347; e-mail: dkmccool@wsu.edu.

ISSN 2151-0032

simulation sites was on a Palouse silt loam soil (fine-silty, mixed mesic pachic Ultic Haploxeroll) about 4 km from the runoff plots at the PCFS. The rainfall simulation study was carried out on 9 July 1987. Within the WEPP model, adjustment is made to the soil erodibility determined from the summer experiments to address changes during other times of the year (Flanagan and Nearing, 1995).

Brooks et al. (2001), following Elliot et al. (1989), calculated WEPP rill erodibility for each of the field-observed runoff and erosion events on the PCFS CBF runoff plots during 1984-1990. Brooks et al. (2001) assumed that runoff from a plot was evenly distributed across the rills, and each rill had a rectangular cross-sectional shape and a constant width and depth ratio. The number of rills in each plot was determined from field photos taken in spring. The authors found that the rill erodibility of frozen soil was much lower than that of unfrozen or thawing soils, and the rill erodibility of thawing and unfrozen soils did not differ significantly.

Van Klaveren and McCool (2010) conducted laboratory measurements of rill erodibility and critical shear on thawed topsoil of the Palouse silt loam at the PCFS using a tilting flume with a radiant freezing plate. They found that the thawed Palouse silt loam soil had a high rill erodibility and low critical shear stress; both rill erodibility and critical shear varied with water potential of the surface soil.

The objective of this study was to evaluate the seasonal changes of the WEPP hydraulic and erosion parameters, including soil effective hydraulic conductivity, critical shear stress, and rill erodibility, especially as impacted by soil freeze and thaw, for two PCFS CBF runoff plots.

Methods and Materials

Laboratory-Measured Erosion Parameters for PCFS Soil

The laboratory experiments by Van Klaveren and McCool (2010) on soils that had been frozen and thawed included nine single-rill erosion tests at three flow rates (approx. 2, 3, and 4 L min^{-1}) with three preset surface soil water tensions (50, 150, and 450 mm) and two additional tests at a low flow rate of approximately 1 L min^{-1} with 50 and 150 mm soil water tensions (Van Klaveren and McCool, 2010). Rill erodibility and critical shear stress were estimated for each surface soil water tension at testing times of 10, 20, 30, 45, 60, and 90 min by fitting the rill detachment capacity equation in the WEPP model (eq. 1):

$$D_c = K_r \left(\tau - \tau_c \right) \quad (1)$$

where D_c is detachment capacity by rill flow (kg s^{-1} m^{-2}), K_r is a rill erodibility parameter (s m^{-1}), τ is flow shear stress acting on the soil particles (Pa), and τ_c is the rill detachment threshold parameter, or critical shear stress, of the soil (Pa). Rill detachment is considered to be zero when flow shear stress is less than the critical shear stress of the soil (Foster et al., 1995).

In each erodibility determination, all soil detachment prior to the specific testing time was included. Thus, the 90 min data included erosion that had occurred from the start

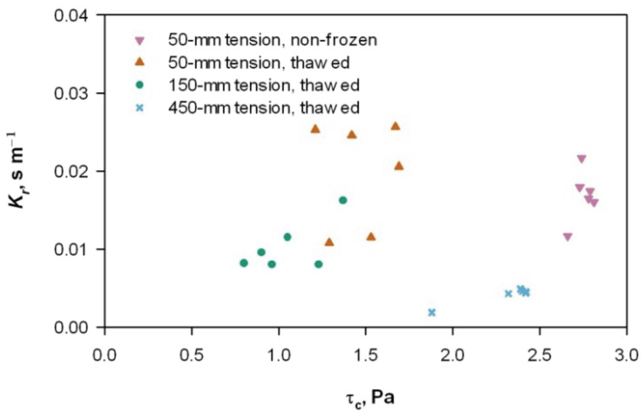

Figure 1. Rill erosion parameters measured in laboratory experiments by Van Klaveren and McCool (2010).

of the test until 90 min. For any tension, K_r was generally the smallest and τ_c the largest at 90 min. It is common for soil erodibility to decline during an experiment, and hence longer experimental times frequently yield lower erodibility values, as shown in previous studies. Foltz et al. (2008) observed this trend from runoff simulation studies on forest roads and developed a relationship between K_r and total event runoff. Elliot et al. (1991), by examining the rill experimental data of Elliot et al. (1989), showed that rill erodibility declined at the higher flow rates that occurred near the end of each rill experiment.

The experiments on thawed soils by Van Klaveren and McCool (2010) covered a wide range of soil water tension: from 50 mm, when the surface is near saturation and the soil is highly susceptible to erosion, to 450 mm, at which point the soil is much less erodible. Van Klaveren and McCool (2010) also reported a separate study with non-frozen soil at 50 mm tension, which resembles summer conditions. The fitted critical shear stress and rill erodibility values from these experiments ranged from 0.80 to 2.81 Pa and from 0.0019 to 0.026 s m^{-1}, respectively (fig. 1). The highly erodible soil has low critical shear stress and high rill erodibility.

Field-Observed Erosion Events on CBF Plots at the PCFS

The PCFS (46° 45′ N, 117° 12′ W) is located 3 km northwest of Pullman, Washington. Long-term experimental runoff plots have been installed at the PCFS since the 1970s (McCool et al., 2002). Data from these experimental plots included weather, snow and frost depths, and runoff and sediment yield from fall 1978 to spring 1991. A 24 h chart-type recording rain gauge near the runoff plots provided break-point rainfall data for this study (Lin and McCool, 2006). Snow depth was measured with snow stakes, and frost depth was measured with frost tubes (McCool and Molnau, 1984) installed at three locations (top, middle, and bottom) along the edge of each plot. The top and bottom depths of the frozen zone were recorded. Runoff and sediment yield were measured using runoff collection tanks and pumps with sample splitters (McCool et al., 2006).

In this study, erosion events observed during 1984-1990

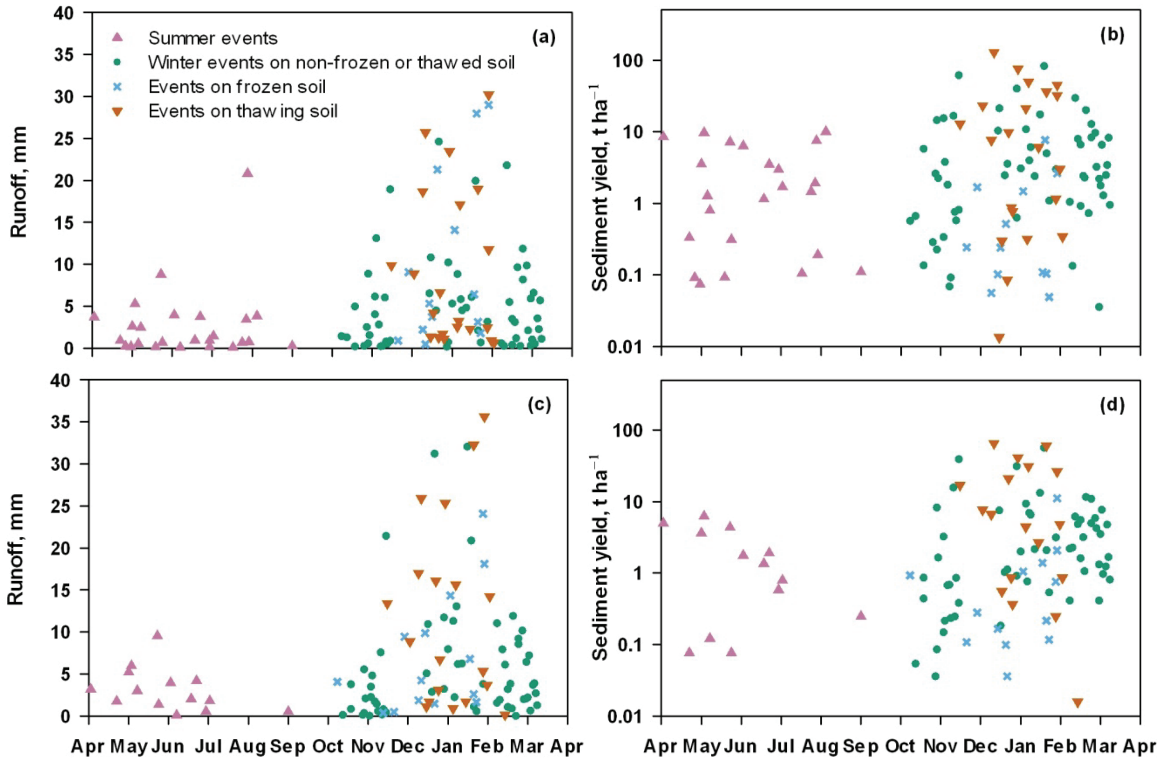

Figure 2. Observed runoff and sediment yield from (a and b) plot 13 and (c and d) plot 36.

on two CBF runoff plots (plots 13 and 36) were used to examine the seasonal changes of WEPP rill erosion parameters. The plots were 22.3 m long and 3.7 m wide on south-facing slopes, 155° and 175° from due north, and with slope gradients of 21.5% and 15.6% for plot 13 and 36, respectively (McCool et al., 2006). The soil on both plots was Palouse silt loam. Plot borders were removed, the plots were tilled, and the borders were replaced during a short period in late September and early October, a low-precipitation period in the area.

The observed runoff and erosion events were classified as the following: summer and early fall events ("summer events" hereafter) that occurred during April to September, and winter and early spring events ("winter events" hereafter) on non-frozen or thawed soil, frozen soil, or thawing soil that occurred during October to March. The soil under the winter condition was categorized as (1) frozen as observed by field personnel before and during the event and by the frost tubes being frozen with no thawing from the top, (2) thawing when frozen soil was observed on the day before the runoff event and partial or complete thaw of the frozen frost tubes was observed on the day of the event, and (3) non-frozen or thawed.

From January 1984 to April 1990, when plot 13 was discontinued, the recorded runoff and erosion events numbered 124 on plot 13 and 116 on plot 36 (fig. 2). Ten summer events were recorded on plot 13 in 1989, while none were recorded on plot 36, as it was not in operation that summer. In addition, there were four events on plot 13 and six on plot 36 that did not occur at the same time. Among the ten mismatched events, one occurred in summer with 0.16 mm of runoff on plot 13, three of the winter events were large, one (1.4 mm) on plot 13 and the other two (4.1 and 11.0 mm) on plot 36, and the remaining six were small, with less than 0.5 mm of runoff. The mismatching of the winter events was likely caused by uneven soil frost, snowmelt, and snow drift across the field. The 110 matched runoff events included 20 summer events and 90 winter events, of which 56 were on non-frozen or thawed soil, 13 on frozen soil, 20 on thawing soil, and one (22 Feb. 1989) on thawing soil on plot 13 and on frozen soil on plot 36. Averages of event runoff and sediment yield for each category are shown in table 1. In general, runoff from the winter events was substantially greater than from the summer events. Similarly, sediment yield from all winter events except those on frozen soil was much greater than from the summer events.

Table 1. Averages of runoff and sediment yield of the matched events on plots 13 and 36.

		Plot 13		Plot 36	
Category	No. of Events	Runoff (mm)	Sediment Yield (t ha^{-1})	Runoff (mm	Sediment Yield (t ha^{-1})
Summer events	20	2.4	3.3	2.9	2.2
Winter events on non-frozen or thawed soil	56	5.2	8.3	5.6	5.5
Winter events on frozen soil	13	9.6	1.1	13.2	0.5
Winter events on thawing soil	20	9.1	20.4	11.6	14.6

ESTIMATING SOIL EROSION PARAMETERS USING FIELD-OBSERVED EVENTS AND WEPP

The WEPP model has been used to estimate infiltration and erosion parameters from rainfall simulation data using the single-storm mode of model application (Copeland and Foltz, 2009; Foltz et al., 2009). A steady-state sediment continuity equation is used in WEPP to describe the movement of sediment in a rill (eqs. 1, 2, and 3; Foster et al., 1995):

$$\frac{dG}{dx} = D_f + D_i \tag{2}$$

$$D_f = D_c\left(1 - \frac{G}{T_c}\right) \tag{3}$$

where G is sediment load (kg s^{-1} m^{-1}), D_i is interrill sediment delivery to the rill (kg s^{-1} m^{-2}), D_f is rill erosion rate (kg s^{-1} m^{-2}), D_c is detachment capacity by rill flow (kg s^{-1} m^{-2}; eq. 1), T_c is sediment transport capacity in the rill (kg s^{-1} m^{-1}), and x is the distance downslope (m).

In the WEPP model, soil rill erodibility and critical shear stress are sensitive parameters in estimating sediment yield from hillslopes to streams. In continuous-simulation mode, τ_c and K_r are adjusted internally to account for soil consolidation with time based on user inputs, e.g., time since tillage, and to account for soil freeze and thaw using adjustment factors. The adjustment factors are calculated based on soil matric potential and are applied when the daily minimum temperature is lower than 0°C or when snow or soil frost is present. In this study, we carried out single-event WEPP simulations without the aforementioned internal adjustment of τ_c and K_r to reproduce the observed runoff and sediment yield for each matched runoff event on plots 13 and 36. Soil effective hydraulic conductivity (K_e) was adjusted to reproduce the observed runoff, and τ_c and K_r were subsequently adjusted to reproduce the observed sediment yield. The resultant τ_c and K_r were regarded as the effective values for each individual event.

Four input files describing climate, topography, soil, and land use and management were developed for the WEPP simulation. The climate inputs included break-point precipitation from the recording rain gauge and snow measurements, and daily maximum and minimum temperatures, wind direction and velocity, humidity, and solar radiation from the NOAA Pullman 2 NW weather station, 0.6 km to the east of the runoff plots. To avoid activating the WEPP internal adjustment of τ_c and K_r, climatic inputs for a typical summer day, except the break-point precipitation for each specific event, were used in each simulation. The break-point precipitation consisted of observed rainfall and estimated snowmelt during each erosion event. Snowmelt was estimated from the changes of the observed snow depth with an assumed snow density of 350 kg m^{-3}. If snowmelt coincided with a rainfall event, the snowmelt was then assumed to be evenly distributed over the rainfall duration; otherwise, it was evenly distributed between 7:00 a.m. and 5:00 p.m.

Soil inputs were those for the Palouse silt loam in the WEPP soil database, with an assumed initial soil saturation of 65% (corresponding to soil water content at field capacity) and the adjusted K_e, τ_c, and K_r. Topographic inputs were a uniform slope configuration, with respective slope gradients and aspects, and the dimensions of plots 13 and 36. The management condition was continuous bare tilled fallow for the PCFS plot (Lin and McCool, 2006).

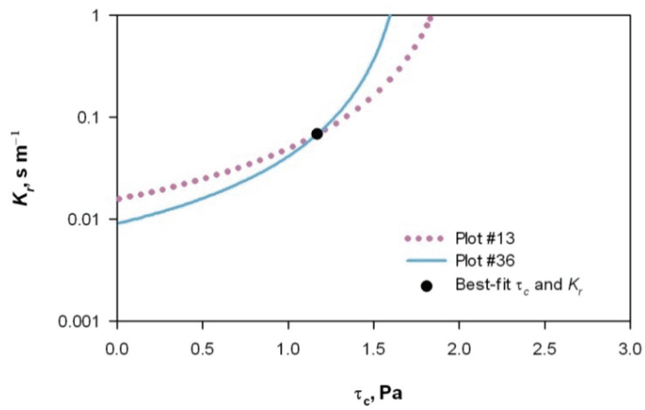

Figure 3. Fitted τ_c and K_r curves with an intersection for the runoff and erosion event on 23 January 1984.

To reproduce an observed runoff, we adjusted K_e following the bisection method. Repeated WEPP runs were made with varied K_e until the difference between the observed and simulated runoff was within a tolerance level of 0.05 mm. Subsequently, we adjusted τ_c and K_r to reproduce sediment yield for the event. Specifically, we changed τ_c from 0.01 Pa to 3.0 Pa (covering the range of τ_c observed for the Palouse silt loam) with an increment of 0.01 Pa, and we obtained the best-fit K_r within 10^{-6} to 10^2 s m^{-1} (covering the observed K_r range) using the bisection method for each τ_c with a tolerance level of 0.05 t ha^{-1} for sediment yield. The resultant τ_c and K_r values for the two plots were plotted for each event, and the values at the intersection of the two K_r vs. τ_c curves were taken as the critical shear stress and rill erodibility for the event. Figure 3 shows an example of the fitting of K_r and τ_c for the runoff and erosion event on 23 January 1984.

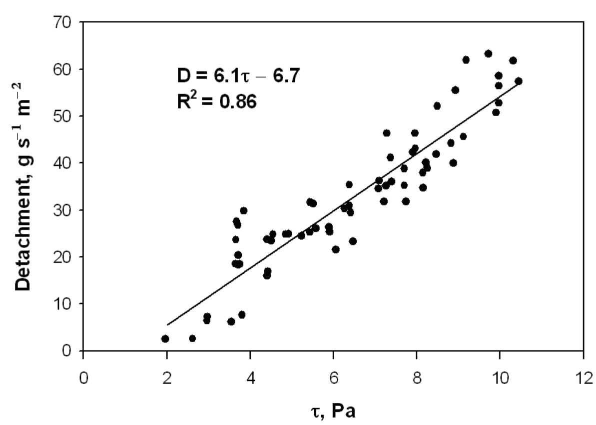

Figure 4. Rill detachment and hydraulic shear for the Palouse silt loam in the rainfall and runoff simulation experiments of Elliot et al. (1989).

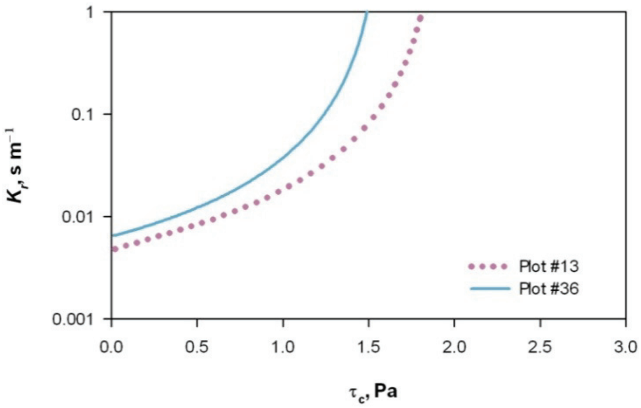

Figure 5. Fitted τ_c and K_r curves without intersection for the runoff and erosion event on 12 December 1984.

Estimating Erodibility with Rainfall Simulation

In the rainfall simulation study by Elliot et al. (1989), rainfall at 62 mm h^{-1} was applied, and rill flows at nominal steps of 10, 20, 30, 40, and 50 L min^{-1} were added. Figure 4 shows the relationship between rill detachment rate and the hydraulic shear calculated for the runoff from the six rills in that study. The critical shear was calculated as 1.1 Pa, and the rill erodibility was calculated as 0.0062 s m^{-1}.

Results and Discussion

Of the 110 matched events, slightly more than half (65) had intersections between the τ_c and K_r curves. For the other 45 events, the two curves diverged from each other and did not have an intersection within the specified parameter ranges. Figure 5 shows one such example. The two-sample t-tests at α = 0.05 with unequal variances showed that, in general, runoff, sediment yield, and sediment yield per mm runoff from the events with or without an intersection do not differ significantly. Thirteen of the 65 events with an intersection were summer events, 35 were winter events on non-frozen or thawed soils, six were on frozen soils, and ten were on thawing soils. The event on 22 February 1989 also had an intersection of the fitted τ_c, and K_r, but the soil conditions were different on the two plots, thawing on plot 13 and frozen on plot 36. Therefore, this event was excluded from the analysis. The following results and discussion were based on the 64 events that had best-fit K_e, τ_c, and K_r values (fig. 6, table 2).

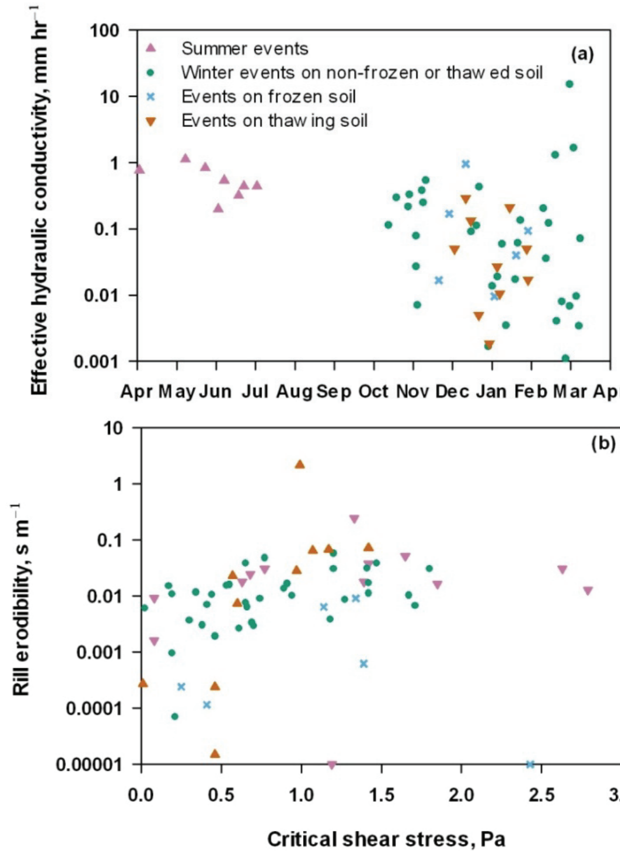

Figure 6. Best-fit (a) effective hydraulic conductivity and (b) critical shear stress and rill erodibility.

The assumed initial saturation level affected the best-fit K_e, but not τ_c and K_r. At the initial saturation of 65%, the mean values of K_e, τ_c, and K_r were, respectively, 0.6 mm h^{-1}, 1.27 Pa, and 0.038 s m^{-1} for summer events; 0.6 mm h^{-1}, 0.80 Pa, and 0.015 s m^{-1} for winter events on non-frozen or thawed soil; 0.2 mm h^{-1}, 1.16 Pa, and 0.0027 s m^{-1} for events

Table 2. Descriptive statistics of the fitted K_e, τ_c, and K_r.

Category	No. of Events	Parameter	Plot 13 Runoff (mm)	Plot 13 Sed. Yield (t ha^{-1})	Plot 13 K_e (mm h^{-1})	Plot 36 Runoff (mm)	Plot 36 Sed. Yield (t ha^{-1})	Plot 36 K_e (mm h^{-1})	τ_c (Pa)	K_r (s m^{-1})
Summer events	13	Mean	2.6	6.8	0.6	3.0	3.7	0.5	1.27	0.038
		SD	2.7	6.3	0.5	2.9	3.5	0.4	0.84	0.060
		Max.	8.8	18.9	1.7	9.5	11.1	1.5	2.79	0.25
		Min.	0.1	0	0.01	0.1	0.03	0.002	0.08	0.00001
Winter events on non-frozen or thawed soil	35	Mean	6.1	20.3	0.7	5.5	11.8	0.6	0.80	0.015
		SD	6.1	34.9	2.7	6.4	24.0	2.4	0.49	0.014
		Max.	24.6	183.9	16.2	31.2	126.5	14.5	1.80	0.058
		Min.	0.2	0.1	0.00001	0.1	0.1	0.0003	0.02	0.00007
Winter events on frozen soil	6	Mean	13.6	5.1	0.3	15.6	1.6	0.1	1.16	0.0027
		SD	12.6	6.3	0.7	14.9	1.7	0.1	0.79	0.0040
		Max.	29.0	17.1	1.7	41.0	4.7	0.3	2.43	0.0091
		Min.	0.5	0	0.01	0.5	0	0.01	0.25	0.00001
Winter events on thawing soil	10	Mean	12.2	77.3	0.1	12.2	39.9	0.1	0.77	0.24
		SD	12.5	97.5	0.1	12.7	50.0	0.1	0.42	0.66
		Max.	32.2	307.7	0.2	35.6	146.3	0.4	1.42	2.13
		Min.	1.3	0.03	0.003	0.9	0	0.0002	0.01	0.00002

on frozen soil; and 0.1 mm h^{-1}, 0.77 Pa, and 0.24 s m^{-1} for events on thawing soils (table 2). A preliminary assessment with different initial saturations showed that the K_e values for the same runoff event category were much lower at the lower initial water saturation. However, the trend of the seasonal changes in the best-fit K_e, τ_c, and K_r was similar under different levels of initial saturation. In general, the initial water content was lower than field capacity for the summer events and higher than field capacity for the winter events on frozen or thawing soil. In the following, we only present the results for the initial saturation level of 65% and focus on τ_c and K_r.

Generally, soils exhibited lower K_e and poorer permeability during the freeze and thaw period. Thawing soil was the most erodible, with a combination of the lowest τ_c and highest K_r in the four runoff event categories, and frozen soil was the least erodible, with a relatively high τ_c and the lowest K_r value. Non-frozen or thawed soil in winter had lower τ_c and K_r values than the soil in summer. Hence, the non-frozen or thawed soil in winter would be more prone to rill initiation than the soil in summer, but the overall erosion may not differ.

For those winter events on non-frozen or thawed soil, the fitted τ_c and K_r values were similar to those of thawed soil under 150 mm tension reported by Van Klaveren and McCool (2010). For the summer events, the fitted τ_c values were lower and the fitted K_r values were higher than the laboratory-measured values for non-frozen soil of Van Klaveren and McCool (2010). Therefore, summer soil would be more erodible in a naturally occurring runoff event than in the laboratory experiment, which may be partially attributed to the raindrop effects on soil erosion.

The fitted τ_c and K_r values for the summer events were both larger than reported by Elliot et al. (1989), likely due to the difference in surface soil conditions in the naturally occurring runoff and erosion events in this study and the rainfall-simulation field experiments of Elliot et al. (1989). For their field experiments, the volumetric water content measured within the top 5 cm of the soil was between 0.07 and 0.17 cm^3 cm^{-3} (saturation level of 11% and 27%, respectively). Under such dry conditions, the Palouse silt loam, with more than 20% clay, can be readily detached due to slaking upon wetting and thus exhibits a low critical shear (Elliot and Laflen, 1993). In addition, the field experiments were carried out within several hours of a tillage operation, which likely resulted in freely available soil particles and aggregates in the rill channel. The low antecedent soil water content may have led to the low rill erodibility values. It should be noted that the rainfall intensity in the Palouse region is much lower than in the rainfall-simulation field experiments of Elliot et al. (1989). Naturally occurring runoff events when the surface soil is dry and freshly tilled are rare in the Palouse region. In addition, tillage operations on the CBF plots were implemented only in late summer in a normally dry period between summer storms and the start of fall precipitation.

The results from the two-sample t-tests at $\alpha = 0.05$ with unequal variances (table 3) indicate that the summer events generated lower runoff than the winter events. However, the means of the fitted K_e do not differ significantly for any two event categories, except between the winter events on thawing soil and the summer events. There was no significant difference in observed runoff among winter events on frozen, thawing, and non-frozen or thawed soil.

Sediment yield from the summer events was lower than from the winter events on thawing and non-frozen or thawed soil, but was not significantly different from that on frozen soil. Sediment yield on frozen soil was significantly lower than on the thawing and thawed or non-frozen soil in winter. There was no significant difference between the observed sediment yield from the thawing and non-frozen

Table 3. Two sample t-tests on K_e, τ_c, and K_r for different runoff event categories.[a]

Test	Parameter	SE/WU	SE/WF	SE/WT	WU/WF	WU/WT	WF/WT
Observed RF	Degree of freedom	44	5	10	5	10	10
	t statistic	-2.33	-2.11	-2.32	-1.56	-1.56	0.35
	t critical one-tail	1.68	2.02	1.81	2.02	1.81	1.81
	P(T <= t) one-tail	0.01	0.04	0.02	0.09	0.07	0.37
Observed SY	Degree of freedom	39	13	9	38	10	9
	t statistic	-2.12	0.98	-2.30	2.48	-1.79	-2.38
	t critical one-tail	1.68	1.77	1.83	1.69	1.81	1.83
	P(T <= t) one-tail	0.02	0.17	0.02	0.009	0.052	0.02
Observed SY/RF	Degree of freedom	26	13	10	37	10	9
	t statistic	-0.66	4.03	-1.61	6.55	-1.42	-2.79
	t critical one-tail	1.71	1.77	1.81	1.69	1.81	1.83
	P(T <= t) one-tail	0.26	<0.001	0.07	<0.001	0.09	0.01
K_e	Degree of freedom	39	12	13	39	34	5
	t statistic	-0.16	1.76	3.68	0.90	1.25	0.88
	t critical one-tail	1.68	1.78	1.77	1.68	1.69	2.02
	P(T <= t) one-tail	0.44	0.052	0.001	0.19	0.11	0.21
τ_c	Degree of freedom	15	10	18	6	17	7
	t statistic	1.87	0.27	1.84	-1.07	0.21	1.12
	t critical one-tail	1.75	1.81	1.73	1.94	1.74	1.89
	P(T <= t) one-tail	0.04	0.40	0.04	0.16	0.42	0.15
K_r	Degree of freedom	12	12	9	30	9	9
	t statistic	1.32	1.99	-0.95	4.09	-1.07	-1.13
	t critical one-tail	1.78	1.78	1.83	1.70	1.83	1.83
	P(T <= t) one-tail	0.11	0.03	0.18	<0.001	0.15	0.14

[a] RF = runoff, SY = sediment yield, SY/RF = sediment yield per mm runoff, SE = summer events, WF = winter events on frozen soil, WT = winter events on thawing soil, and WU = winter events on non-frozen or thawed soil.

or thawed soil. Sediment yield per mm runoff did not differ between the summer events and winter events on thawing and non-frozen or thawed soil, but was significantly greater than that from frozen soil.

The τ_c values for the summer events were significantly greater than for the winter events on thawing and non-frozen or thawed soil. There was no significant difference in the means of τ_c in all the remaining comparisons. The frozen soil had significantly lower rill erodibility than the soil in summer and the non-frozen or thawed soil in winter, as reported by Brooks et al. (2001). However, no significant difference was found in the rill erodibility of frozen and thawing soil.

The adjustment factors for critical shear stress and rill erodibility for frozen soil in the WEPP model are functions of matric potential of the surface soil (eqs. 5 and 6; Alberts et al., 1995):

$$C\tau_{cft} = 0.875 + 0.0543 \times \ln\left(\psi_{surf}\right) \tag{5}$$

$$CK_{rft} = 2.0 \times 0.933^{\Psi_{surf}} \tag{6}$$

where $C\tau_{cft}$ is the adjustment factor for freeze-thaw effects for critical shear stress, CK_{rft} is the adjustment factor for rill erodibility, and Ψ_{surf} is the matric potential of the surface soil (kPa). During a simulated freeze-thaw cycle, the adjustment is deactivated when the transient soil water content is lower than the soil water content at field capacity, and will be activated at the next freeze-thaw cycle.

CK_{rft} is 0.2 at field capacity and reaches 2.0 at saturation. $C\tau_{cft}$ is 1.1 at field capacity and decreases sharply as soil water content approaches saturation (fig. 7). The ratio of the K_r value for the thawing soil to the K_r value for the summer soil from this study is 6.3 (table 2), which is out of the range of the CK_{rft} values in WEPP. Provided that the surface soil tension can be estimated adequately, $C\tau_{cft}$ based on equation 5 would be 1.09 for equation 6 to produce a CK_{rft} value of 0.07, as estimated in this study for the frozen soil. However, $C\tau_{cft}$ from the best-fitted τ_c values was 0.91. Similarly, $C\tau_{cft}$ estimated using equation 5 would be 1.04 for equation 6 to produce a CK_{rft} value of 0.39, as estimated for the winter non-frozen or thawed soil. In comparison, the estimated $C\tau_{cft}$ value was 0.63 in this study.

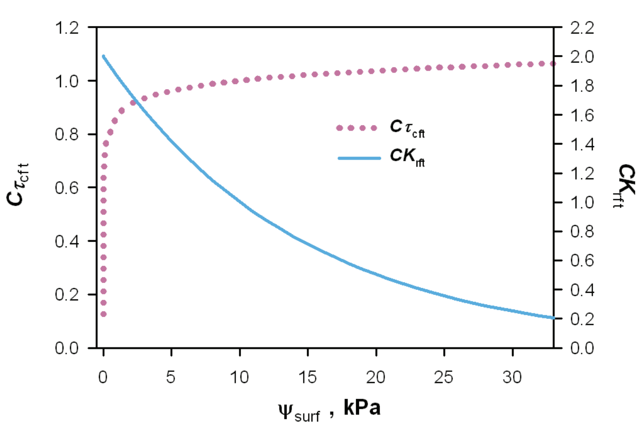

Figure 7. Adjustment factors for τ_c and K_r for soil freeze and thaw in the WEPP model.

Figure 8 shows the changes in τ_c and K_r with matric potential from Van Klaveren and McCool (2010) and the changes in $C\tau_{cft}$ and CK_{rft} with matric potential as the surface soil approaches saturation. The regression line for K_r is nearly parallel to the CK_{rft} curve, suggesting that CK_{rft} may be used to represent the changes in K_r for thawing soil. For fitting τ_c, a second-order regression model was superior to the first-order model at a significant level of $\alpha = 0.05$ with a p-value less than 0.001 from an F-test following Sokal and Rohlf (1995):

$$\mathrm{F} = \frac{(\mathrm{SSE}_1 - \mathrm{SSE}_2)/df1}{\mathrm{SSE}_2/df2} \tag{7}$$

where SSE_1 and SSE_2 are the sums of the residual squares for the regression models of first and second order, respectively, $df1$ is the number of extra terms in the second-order model, and $df2$ is the residual degrees of freedom for the second-order model. The $C\tau_{cft}$ curve in the current WEPP is convex, different from the concave regression curve (fig. 8). The adjustment method for rill erosion parameters in the WEPP model may need to be modified to reflect the dynamic changes induced by soil freeze and thaw.

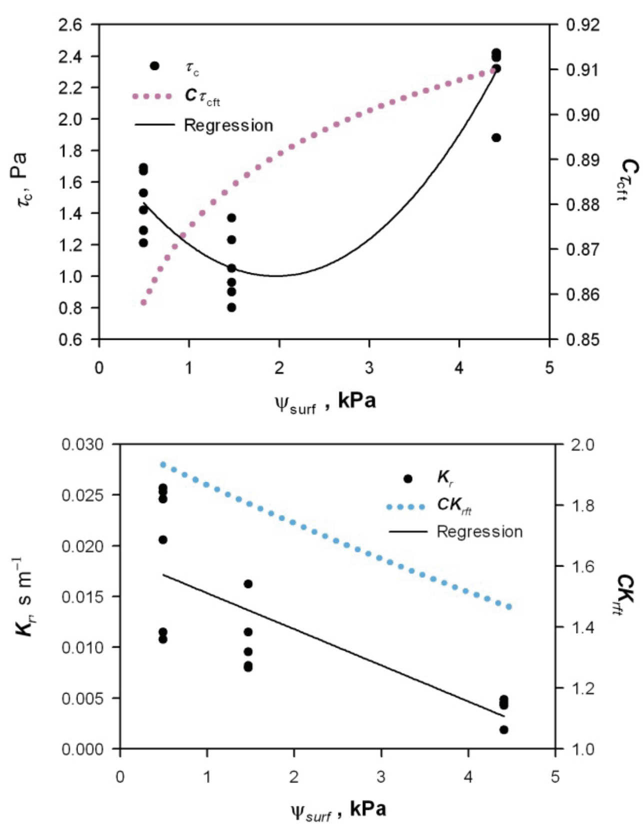

Figure 8. Laboratory-measured τ_c and K_r for thawed Palouse silt loam soil (Van Klaveren and McCool, 2010) and adjustment factors for τ_c and K_r for soil freeze and thaw as soil approaches saturation in the WEPP model.

SUMMARY

Field-observed runoff and soil erosion events on two continuous bare tilled fallow runoff plots at the Palouse Conservation Field Station (PCFS) in southeastern Washington in the U.S. Pacific Northwest were used to best fit water erosion parameters (rill erodibility and critical shear stress) for each event using the WEPP model. The observed erosion events were categorized into summer events, winter events on frozen soil, winter events on thawing soil, and winter events on non-frozen or thawed soil to examine the seasonal changes in the erosion parameters. For frozen soil, τ_c was 0.91 times and K_r was 0.07 times the values for summer soil; for thawing soil, τ_c was 0.61 times and K_r was 6.3 times the values for summer soil; and for non-frozen or thawed soil, τ_c was 0.63 times and K_r was 0.39 times the values for summer soil. The adjustment factor in WEPP for τ_c for soil freeze and thaw appeared inadequate for describing the seasonal changes in τ_c, especially for the winter events on non-frozen or thawed soil. The adjustment method for rill erosion parameters in WEPP may need to be modified to reflect the dynamic changes induced by soil freeze and thaw processes. Future studies are needed to further examine site-specific conditions, such as microclimate and spatial variation in soil properties, to better understand seasonal changes in soil erodibility. Efforts are also needed to assess the impacts of crop cover and surface residue on soil freeze and thaw in cold regions to develop systematic and sound approaches to adjusting the erodibility parameters in the WEPP model.

REFERENCES

Alberts, E. E., M. A. Nearing, M. A. Weltz, L. M. Risse, F. B. Pierson, X. C. Zhang, J. M. Laflen, and J. R. Simanton. 1995. Soil component. In *USDA Water Erosion Prediction Project Hillslope Profile and Watershed Model Documentation*, 7.1-7.47. D. C. Flanagan and M. A. Nearing, eds. NSERL Report 10. West Lafayette, Ind.: USDA-ARS National Soil Erosion Research Laboratory.

Brooks, E. S., D. K. McCool, and J. Boll. 2001. Determining erodibility parameters for a Palouse silt loam using runoff plot data. In *Proc. Intl. Symp.: Soil Erosion Research for the 21st Century*, 591-594. J. C. Ascough and D. C. Flanagan, eds. St. Joseph, Mich.: ASAE.

Copeland, N. S., and R. B. Foltz. 2009. Improving erosion modeling on forest roads in the Lake Tahoe basin: Small plot rainfall simulations to determine saturated hydraulic conductivity and interrill erodibility. ASABE Paper No. 095553. St. Joseph, Mich.: ASABE.

Dun, S., J. Q. Wu, D. K. McCool, J. R. Frankenberger, and D. C. Flanagan. 2010. Improving frost-simulation subroutines of the Water Erosion Prediction Project (WEPP) model. *Trans. ASABE* 53(5): 1399-1411.

Elliot, W. J., and J. M. Laflen. 1993. A process-based rill erosion model. *Trans. ASAE* 36(1): 65-72.

Elliot, W. J., A. M. Liebenow, J. M. Laflen, and K. D. Kohl. 1989. A compendium of soil erodibility data from WEPP cropland soil field erodibility experiments, 1987 and 1988. NSERL Report 3. West Lafayette, Ind.: USDA-ARS National Soil Erosion Research Laboratory.

Elliot, W. J., A. V. Elliot, J. Q. Wu, and J. M. Laflen. 1991. Validation of the WEPP model with rill erosion plot data. ASAE Paper No. 912557. St. Joseph, Mich.: ASAE.

Flanagan, D. C., and S. J. Livingston, eds. 1995. USDA Water Erosion Prediction Project: User Summary. NSERL Report 11. West Lafayette, Ind.: USDA-ARS National Soil Erosion Research Laboratory.

Flanagan, D. C., and M. A. Nearing, eds. 1995. *USDA Water Erosion Prediction Project Hillslope Profile and Watershed Model Documentation*. NSERL Report 10. West Lafayette, Ind.: USDA-ARS National Soil Erosion Research Laboratory.

Flanagan, D. C., J. E. Gilley, and T. G. Franti. 2007. Water Erosion Prediction Project (WEPP): Development history, model capabilities, and future enhancements. *Trans. ASABE* 50(5):1603-1612.

Foltz, R. B., H. Rhee, and W. J. Elliot. 2008. Modeling changes in rill erodibility and critical shear stress on native surface roads. *Hydrol. Proc.* 22(24): 4783-4788.

Foltz, R. B., N. S. Copeland, and W. J. Elliot. 2009. Reopening abandoned forest roads in northern Idaho, USA: Quantification of runoff, sediment concentration, infiltration, and interrill erosion parameters. *J. Environ. Mgmt.* 90(8): 2542-2550.

Foster, G. R., D. C. Flanagan, M. A. Nearing, L. J. Lane, L. M. Risse, and S. C. Finkner. 1995. Hillslope erosion component. In *USDA Water Erosion Prediction Project Hillslope Profile and Watershed Model Documentation*, 11.1-11.12. D. C. Flanagan and M. A. Nearing, eds. NSERL Report 10. West Lafayette, Ind.: USDA-ARS National Soil Erosion Research Laboratory.

Horner, G. M., A. G. McCall, and F. G. Bell. 1944. Investigations in erosion control and the reclamation of eroded land at the Palouse Conservation Experiment Station, Pullman, Washington, 1931-1942. Tech. Bulletin 860. Washington, D.C.: USDA-SCS.

Kok, H., and D. K. McCool. 1990. Quantifying freeze/thaw induced variability of soil strength. *Trans. ASAE* 33(2): 501-506.

Lin, C., and D. K. McCool. 2006. Simulating snowmelt and soil frost depth by an energy budget approach. *Trans. ASABE* 49(5): 1383-1394.

McCauley, C. A., D. M. White, M. R. Lilly, and D. M. Nyman. 2002. A comparison of hydraulic conductivities, permeabilities, and infiltration rates in frozen and unfrozen soils. *Cold Region Sci. Tech*. 34(2): 117-125.

McCool, D. K., and M. Molnau. 1984. Measurement of frost depth. In *Proc. Western Snow Conf*., 33-41. Western Snow Conference.

McCool, D. K., G. R. Foster, A. H. Ingersoll, R. C. McClellan, and R. W. Rickman. 2002. Cover-management enhancements for RUSLE2 in the Pacific Northwest USA. In *Proc. 12th ISCO Conf*., 513-517. L. Wang, D. Wu, X. Tu, J. Nie, eds. International Soil Conservation Organization. Available at: http://tucson.ars.ag.gov/isco/isco12/VolumeII/Cover-ManagementEnhancements.pdf. Accessed January 2013.

McCool, D. K., K. E. Saxton, and P. K. Kalita. 2006. Winter runoff and erosion on northwestern USA cropland. ASABE Paper No. 062190. St. Joseph, Mich.: ASABE.

Seyfried, M. S., and G. N. Flerchinger. 1994. Influence of frozen soil on rangeland erosion. In *Variability of Rangeland Water Erosion Processes*, 67-82. Special Publication 38. Madison, Wisc.: SSSA.

Sokal, R. R., and F. J. Rohlf. 1995. *Biometry: The Principles and Practice of Statistics in Biological Research*. 3rd ed. New York, N.Y.: W.H. Freeman.

Van Klaveren, R. W., and D. K. McCool. 2010. Freeze-thaw and water tension effects on soil detachment. *SSSA J*. 74(4): 1327-1338.

Zuzel, J. F., R. R. Allamaras, and R. N. Greenwalt. 1982. Runoff and soil erosion on frozen soil in northeastern Oregon. *J. Soil Water Cons*. 37(6): 351-354.